



OPEN

Multicolor iLIFE (m-iLIFE) volume cytometry for high-throughput imaging of multiple organelles

Prashant Kumar¹ & Partha Pratim Mondal^{1,2✉}

To be able to resolve multiple organelles at high throughput is an incredible achievement. This will have immediate implications in a range of fields ranging from fundamental cell biology to translational medicine. To realize such a high-throughput multicolor interrogation modality, we have developed a light-sheet based flow imaging system that is capable of visualizing multiple sub-cellular components with organelle-level resolution. This is possible due to the unique optical design that combines an illumination system comprising two collinear light sheets illuminating the flowing cells and a dedicated dual-color 4f-detection, enabling simultaneous recording of multiple organelles. The system PSF sections up to 4 parallel microfluidic channels through which cells are flowing, and multicolor images of cell cross-sections are recorded. The data is then computationally processed (filtered using ML algorithm, shift-corrected, and merged) and combined to reconstruct the 3D multicolor volume. System testing is conducted using multicolor fluorescent nano-beads (size ~ 175 nm) and flow-based imaging parameters (PSF size, motion-blur, flow rate, frame rate, and number of cell-sections) are determined for quality imaging. Drug treatment studies were carried out for healthy and cancerous HeLa cells to check the performance of the proposed system. The cells were treated with a drug (Vincristine, which is known to promote mitochondrial fission in cells), and the same is compared with untreated control cells. The proposed multicolor iLIFE system could screen ~ 800 cells/min (at a flow speed of 2490 μm/s), and the drug treatment studies were carried out up to 24 h. Studies showed the disintegration of mitochondrial network and dysfunctional lysosomes and their accumulation at the cell membrane, which is a clear indication of cell apoptosis. Compared to control cells (untreated), the mortality is highest at a concentration of 500 nM post 12 h of drug treatment. With the capability of multiorganelle interrogation and organelle-level resolution, the multicolor iLIFE cytometry system is suitably placed to assist optical imaging and biomedical research.

Light sheet technique is shaping several fields ranging from biological to physical sciences^{1,2}. In biology, the technique is heavily used and modernized for the size, shape, and transparency of the specimen, ranging investigation from a single cell to mammalian organs. Prominent light sheet techniques that have accelerated biology and medical research include, SPIM, DSLM, OCPI, diSPIM, LLSM, MLSM, IML-SPIM, light field microscopy, among others^{3–16}. Recent advances have been in physical sciences with applications in lithography, beam-shaping, flow cytometry, particle image velocimetry, plasma physics and optical tweezers^{16–28}. The field is expanding and advancing a wide range of research disciplines that lie at the interface of natural and biomedical sciences¹.

Although the technique was founded in the early twentieth century by Siedentopt and Zsigmondy³⁰, the actual progress started with its rediscovery in 1993 by Voie et al for biomedical imaging³¹. The potential was quickly realized by Stelzer who carried out the first study in developmental biology, and later on, popularized the technique^{32–34}. However, the first light sheet cytometry on a microfluidic platform was first realized by our group in the year 2013²⁶. This seeded the progress of light sheet cytometry in the subsequent years and led to the development of key variants of the iLIFE system dedicated to organism imaging^{27,28}. During the same time, Lau et al reported light sheet based optofluidic time-stretch imaging for high throughput interrogation of MIHA cells³⁵. An exciting development is the on-chip cytometry realized by integrating light sheet on a mirror-embedded microfluidic chip³⁶. Other variants include a scanned Bessel beam for stem cell research, and a label-free imaging flow cytometry for cell screening^{37,38}. Along similar lines, Jiang et al have demonstrated cytometry by integrating droplet microfluidics and light sheet³⁹. In another development, successful imaging of large live

¹Mondal Lab, Department of Instrumentation and Applied Physics, Indian Institute of Science, Bangalore 560012, India. ²Centre for Cryogenic Technology, Indian Institute of Science, Bangalore 560012, India. ✉email: partha@iisc.ac.in

organisms (such as, *C elegans*) is achieved by iLIFE imaging cytometry^{28,31} and SCAPE, especially at high speed⁴⁰. The developments continued, with our group succeeding in high speed interrogation of cells using a single light sheet¹⁶, and Ben-Yakar group using a line excitation array detection (LEAD) fluorescence microscopy for mega-Hertz line-scanning using a virtual light sheet⁴¹. Recently, our group proposed a multifunctional light sheet cytometry system that employs vertically-aligned multi-sheet array (VAMSA) illumination⁴¹. Several other developments are reported in the field demonstrating the potential of light sheet in imaging cytometry. Here, we report the development of light sheet based multicolor iLIFE cytometry system for cell biology and biomedical research. With existing point-illumination based techniques, it is quite evident that the field of cytometry needs a revolution at the fundamental level for it to address the needs of modern biology and biomedical imaging. The bottleneck with existing cytometry is its complex instrumentation, limited functionalities, and bulky design. The existing cytometry techniques use point-illumination for interrogating cells and require two fluids, specimen flowing fluid along with a sheath fluid for hydrodynamic focussing of the specimens^{43,44}. This necessitates colineating cells for sequential interrogation. The arrangements are technically challenging, quite cumbersome, and necessitate trained intervention for optimal performance. Moreover, the existing systems are not suitable for specimens of different kinds (shapes and sizes). However, existing cytometry techniques have found diverse applications in medical health care and biomedical research^{45–54}. To meet the ever-growing demand in medical science, existing techniques need to overcome the new challenges. One of the key obstacles of the existing cytometry is its inability to decipher sub-cellular structures of flowing cells and is not suitable for investigating multiple organelles. This needs optical cross-sectioning, high resolution, and multicolor imaging. Specifically, the use of light sheet for cytometry comes with key advantages such as large field-of-view (suitable for cross-sectioning imaging of large specimens), selective plane interrogation, uniform illumination, high contrast, and better signal-to-background ratio (SBR)⁵⁵. Concerning our previous report where we carried out single-color light sheet based volume flow cytometry (VFC)¹⁶, the present technique advances the technique to multicolor regime where two different organelles can be simultaneously imaged during flow. Specifically, the multicolor light sheet flow cytometry system requires two different light sources to realize multicolor lightsheet PSF, and the detection is carried out by a dual channel 4f optical sub-system. In addition, m-iLIFE system needs labeling of multiple organelles with spectrally-separated emission spectrum, and the data analysis requires additional operations (signal separation, deconvolution, shift-correction, merging, and stacking) to generate multicolor volume images.

In this work, we report a multicolor integrated lightsheet imaging and flow-based enquiry (m-iLIFE) imaging cytometry system for multi-organelle investigation of a large pool of cells. The system is based on multicolor light sheet illumination and dedicated dual-color detection. It was calibrated and tested using a known test sample (a mix of two fluorescent beads suspended in distilled water with a well-separated emission spectrum).

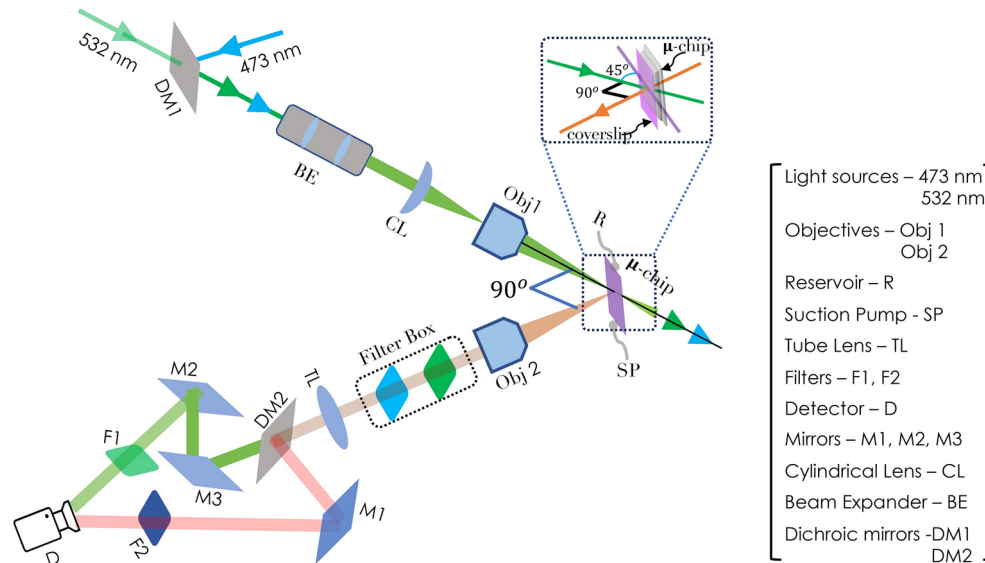


Figure 1. Schematic diagram of the proposed *multicolor – iLife* system. The illumination and detection optical arms are orthogonal to each other. This configuration facilitates a sectional view of flowing cells. The illumination is a combined light sheet that comprises two independent laser beams of wavelengths, 473 nm and 532 nm. The beams are combined using a dichroic mirror (DM1) and expanded 5X times using a beam-expander. The beam is then subjected to a cylindrical lens-objective lens combination to generate diffraction-limited light sheets. These cells flowing through the microfluidic channels are sectioned by the light sheet at high throughput. The fluorescence from the cells (stained with two distinct markers) is collected by the detection arm, filtered (filter box), and separated by a dichroic mirror (DM2). The light is then focussed by an auto-tunable tube lens (TL) on different parts of sCMOS detector chip using a set of mirrors (M1, M2, M3). On its way, additional filters are used to filter out background and stray light. The microfluidic chip is placed at an angle of 45° with respect to illumination lightsheet. The same is explicitly shown in the inset sub-figure.

A commercially viable microfluidic chip with a Y-type channel is fabricated and critical flow parameters are determined for optimal operation. Subsequently, the system is used to study live cell samples (HeLa cells). In specific, drug (Vincristine) treatment studies were carried out and their impact on two different organelles (Mitochondria and Lysosomes labeled with Mitotracker Orange and Lysotracker dyes) were accessed for a large cell population. Moreover, the system enables the determination of critical biophysical parameters related to cell physiology, along with the visualization of organelle distribution in a 3D HeLa cell.

Results

In recent years, light sheet techniques have matured and are now finding applications in diverse research disciplines. Among others, imaging flow cytometry has benefited tremendously with the arrival of light sheet. The fact that illumination can be achieved using a sheet of light instead of existing point PSF has opened up several avenues and greatly enhanced the capability of existing imaging flow cytometry.

Optical setup of multicolor iLIFE volume cytometry system

At the heart of the proposed multicolor iLIFE volume cytometry system is light sheet based illumination sub-system as shown in Fig. 1. The system integrates three sub-systems: multicolor light sheet illumination, microfluidic specimen flow platform, and multicolor 4f fluorescence detection.

The illumination subsystem comprises two distinct light sources of wavelengths, 473 nm and 532 nm, which are combined by a beam combiner (dichroic mirror). The beams are then expanded 5X times using a combination of biconvex lenses to fill the back-aperture of the cylindrical lens. This ensures the use of maximum aperture angle of the cylindrical lens. Since a cylindrical lens is known to focus in one of the lateral axes (say, x-axis), this produces a near-line focus at the back focal-plane of the objective lens. The lens performs a 2D Fourier transform, thereby producing a tightly-focussed diffraction-limited light sheet along the y-axis at the working distance of the objective lens. The illumination PSF (diffraction-limited) is used to section the objects flowing through the microfluidic channel.

Figure 1 inset shows the optical configuration where the illumination and detection sub-systems are placed at 90 degrees to each other. However, the microfluidic chip is placed at 45 degrees with respect to the illuminating light sheet. In addition, the detection is carried out by a dual-channel 4f optical configuration. This combination of 45-degree illumination and detection facilitates the capture of cross-sectional images of the target organelles

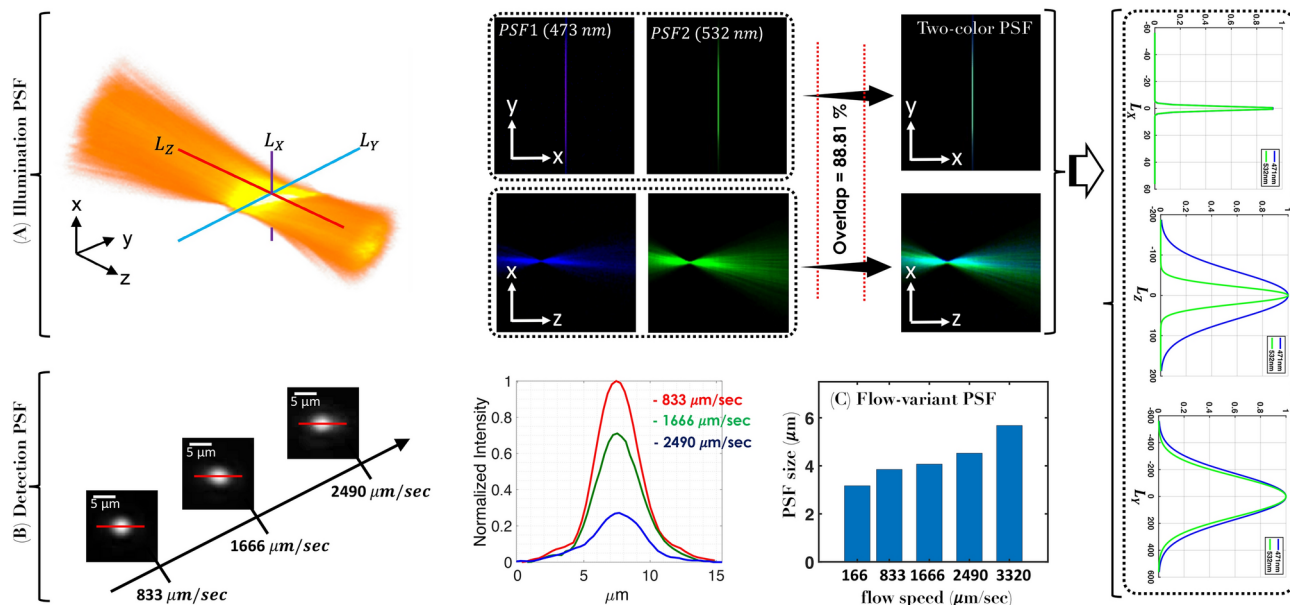


Figure 2. Characterization of System PSF: (A) The characterization of the light sheet field is carried out using a CCD camera, which is scanned in steps of 10 microns at and around the focus of the objective lens to record the illumination field intensity. The corresponding 3D and 2D views of the PSFs (PSF1 and PSF2) are shown along with a two-color field. Both the PSFs have an overlap region of 88.81% which can be used to illuminate the cells flowing through the microfluidic chip. The line intensity plots of the field along X, Y, and Z are used to determine the size of the light sheets. The measured dimension of the system PSF ($L_x \times L_y \times L_z$) is, $(3.75 \times 125 \times 500 \mu\text{m}^3)$. (B) The detection flow-variant PSF at varying flow-speed (833–2490 $\mu\text{m/s}$). Fluorescent beads (diameter = 1 μm) are used as point emitter sources to determine detection PSF. The blur effect due to flow results in a change in PSF (measured in terms of FWHM) as a function of flow rate. The corresponding intensity plot (along the red line) is also shown. The PSF is used for image deconvolution. (C) Flow variant PSFs at varying flow-speed (166–3320 $\mu\text{m/s}$). The calculations are based on a $100 \mu\text{m} \times 100 \mu\text{m}$ channel size, and with the assumption that the flow is laminar and incompressible.

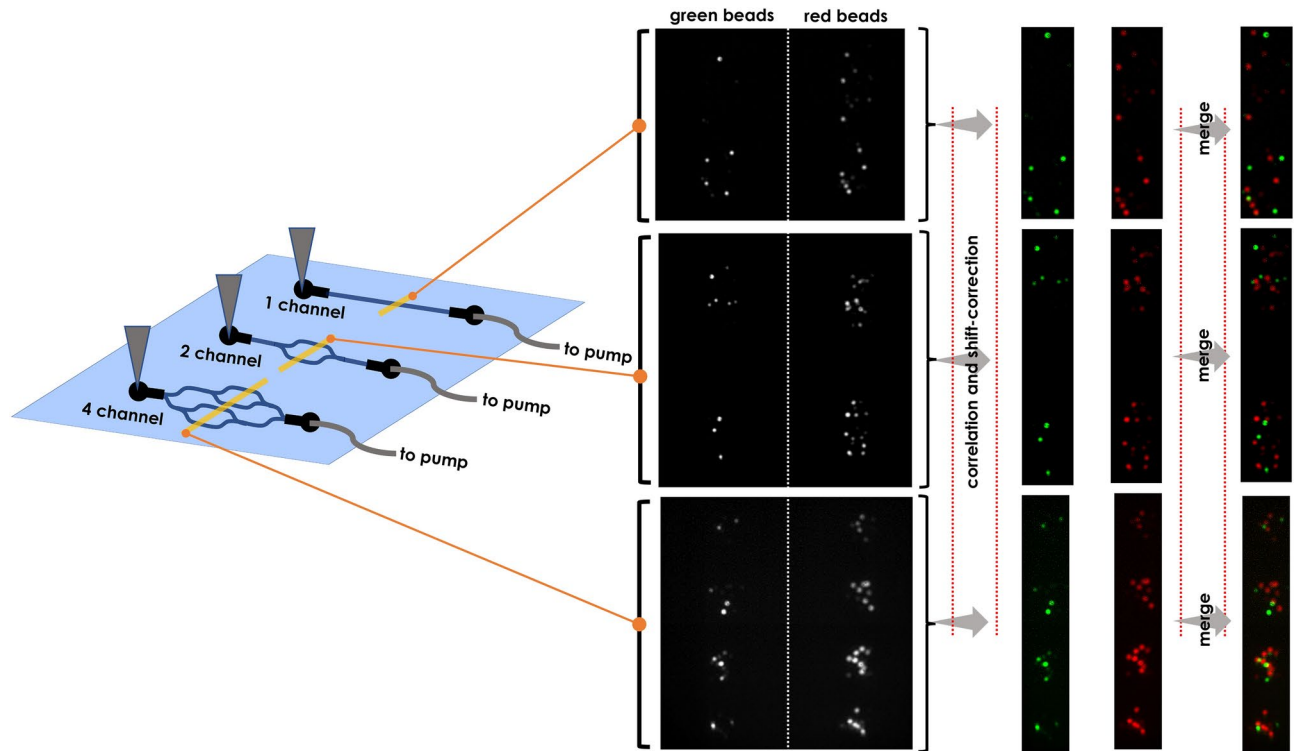


Figure 3. Simultaneous multichannel and Multicolor Visualization: Fluorescent beads are flown through varying microfluidic channel types (1, 2, and 4 channels). Fluorescence (Green channel (left) and Red channel (right)) from two separate optical arms are recorded in two parts of the camera chip. Beads flowing through the microfluidic channels are simultaneously illuminated by the multicolor light sheet and imaged by a fast Zyla4.2-sCMOS camera.

in the cells flowing through the microfluidic channels. Subsequently, the sectional images are deconvolved, shift-corrected, and stacked together to reconstruct the 3D volume of the flowing cells.

The specimen flow sub-system consists of a microfluidic chip, a cell reservoir, and a flow pump. One end of the microfluidic channel is connected to the cell reservoir and the other end to the flow pump. For imaging, the cells are loaded in the reservoir, and the flow pump is operated in suction mode to maintain laminar flow. The flow in the channels is regulated by interfacing software. A channel size of $100 \times 100 \mu\text{m}^2$ ensures a smooth flow of cells that are of size, $15 \mu\text{m}$. The flow is regulated such that the detector can capture ~ 5 planes per cell. Two different organelles (here, mitochondria and lysosomes) are labeled by two fluorophores with distinct absorption and emission spectra. The fluorescence from cells is collected by the detection sub-system.

The detection is achieved by a 4f dual-channel widefield optical sub-system as shown in Fig. 1. The detection sub-system is placed orthogonal to the illumination arm to ensure capture of fluorescence from cell cross-sections as it is transected by the sheet of light. The fluorescence is collected by the detection objective, and directed to the filter box (notch and high-pass filters). Since the emissions are from two different organelles labeled with two distinct fluorophores with well-separable emission maximum (Mitotracker Red FM, Ex/Em = 581/644 nm, and Lysotracker Green DND-26, Ex/Em = 504/511 nm), the fluorescence is split into two different channels by the dichroic mirror (DM2) and directed to two separate parts of the camera chip by a set of mirrors (M1, M2, M3). The mirrors are arranged in such a configuration to easily match the distance between the tube lens (TL) and the detector (D) for both paths. Along each path, additional filters (F1 and F2) are used to filter out background and stray light.

PSF characterization for multicolor iLIFE system

The system requires characterization of the system PSF which is used for interrogating multiple organs in cells flowing at high speed. So, the characterization of the system PSF becomes essential for the realization of multicolor iLIFE system. Figure 2 shows a 2D view of the system PSF along with the 3D volume. The multicolor field was recorded by translating a camera at and about the focus of the objective lens. The optical field is measured in a sequential manner. First, the field is recorded for the blue light (473 nm) by translating the camera along optical path in steps of $10 \mu\text{m}$. The same process is carried out for the second beam (532 nm). The corresponding PSFs are shown in Fig. 2A. The fields are then superimposed to obtain the system PSF. Corresponding intensity plots are also shown for both individual and combined PSFs. The same process is repeated for all z-positions about the focal plane ($-100 \mu\text{m} \leq z \leq +100 \mu\text{m}$). The images are then stacked together to reconstruct the 3D volume of the multicolor light sheet field as shown in Fig. 2A. Visual inspection and corresponding intensity analysis show a high degree of overlap ($\sim 88.81\%$). The dimensions of the multicolor light sheet are, $L_x = 3.75 \mu\text{m}$

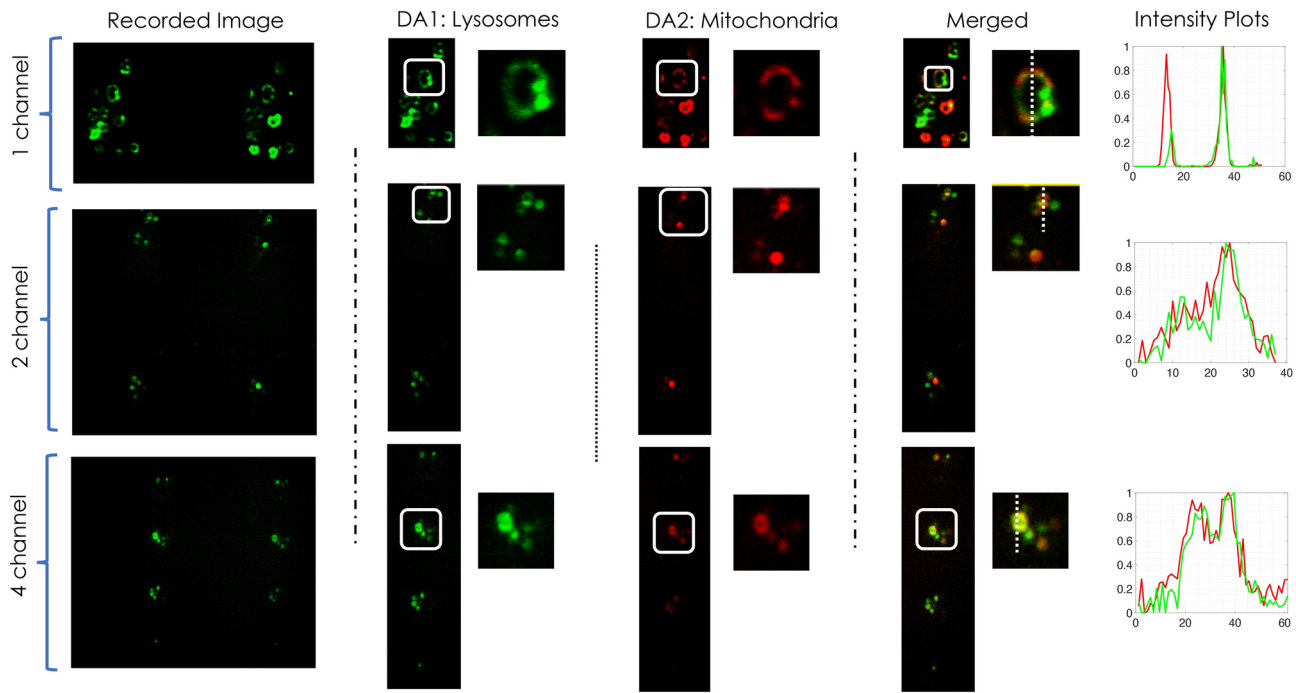


Figure 4. Simultaneous Imaging of Lysosomal and Mitochondrial distribution in HeLa cells: Lysosomes (left channel, DA1) and Mitochondria (right channel, DA2)-labeled HeLa cells are allowed to flow through all the channels and are simultaneously imaged in parallel as they pass through the light sheet, producing sectional images. Fluorescence from both the channels (DA1 and DA2) are merged to reconstruct the 2D multicolor image, showing the distribution of lysosome and mitochondria in the flowing cell. The corresponding intensity plots show intracellular variations of the lysosomes and the mitochondrial network.

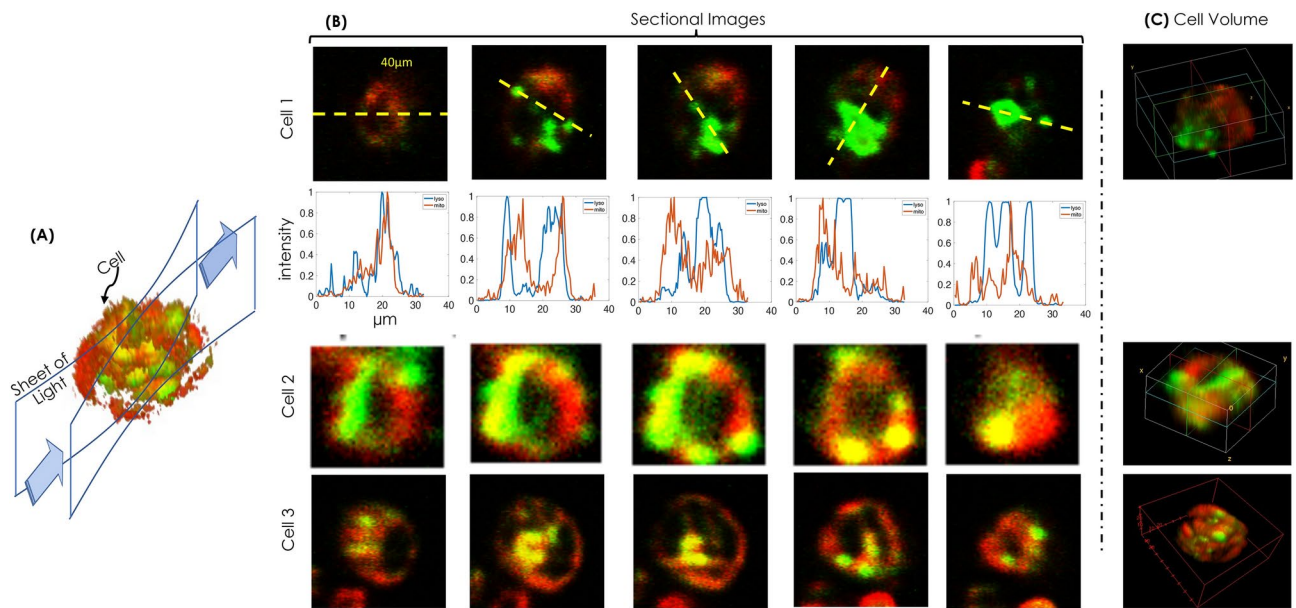


Figure 5. Sectional Images of HeLa cells: (A) A representation showing cells sectioned by light sheet. (B) HeLa cells are flown through the microchannels. The system PSF illuminates the flowing cells and cross-sectional images are recorded by the detection arms. Window 1 (green) represents the set of sectional images with lysosomal distribution and window 2 (red) shows the mitochondrial distribution in a sample cell. Both images are, normalized and merged with the shift corrections to visualize multiple organelles distribution in a 3D cell.

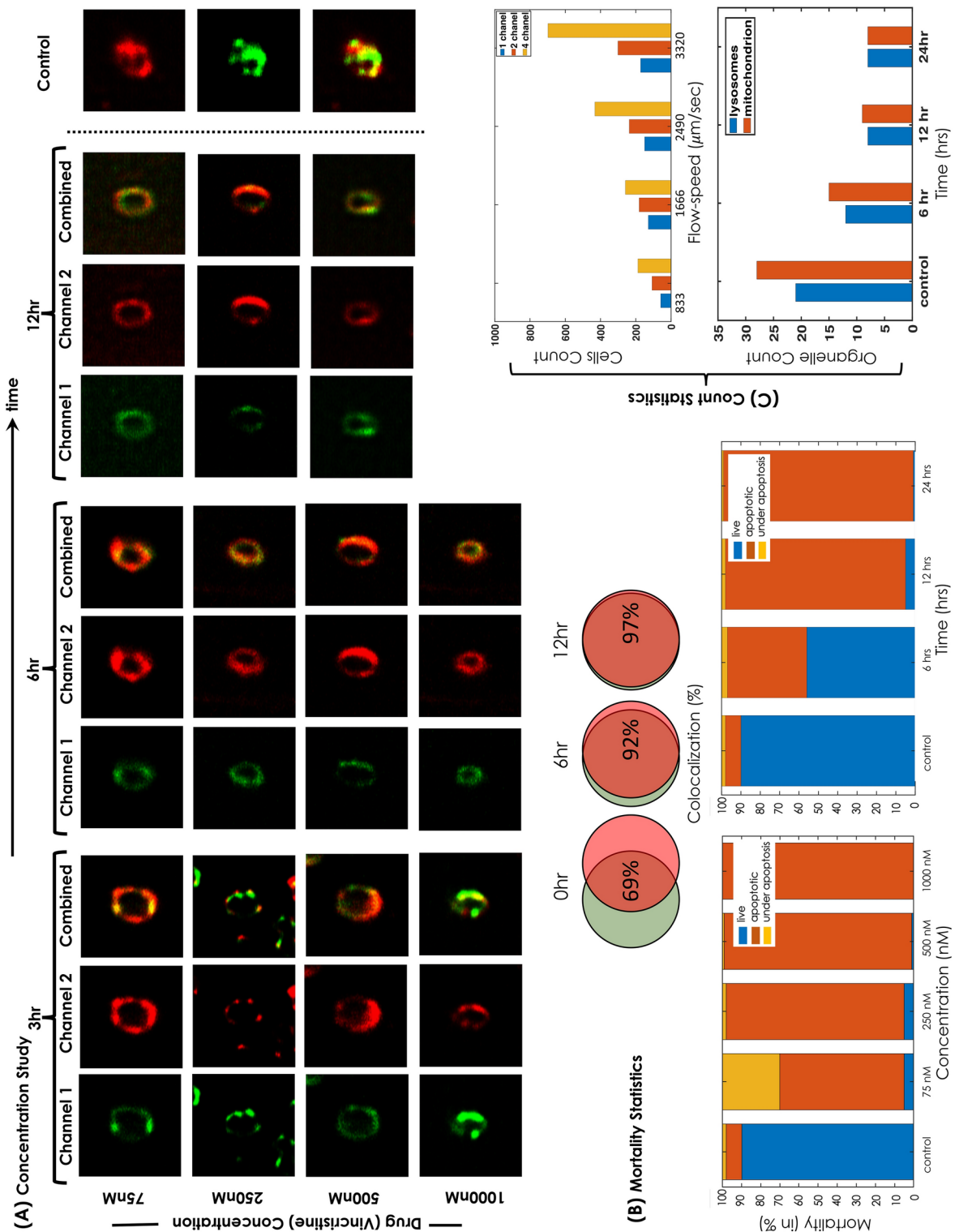


Figure 6. Cell treatment & statistical analysis: HeLa cells are treated with Vincristine at varying concentrations ranging from low (75 nM) to high (1 μ M). m-iLIFE images show mitochondrial and lysosomal distribution throughout the cell cytoplasm. Corresponding images of control cells (0 hrs) are also shown. Images at increasing time points show a decrease in the cell size indicating apoptotic arrest. In addition, the accumulation of organelles (mitochondria and lysosomes) at the peripheral cell membrane is quite evident. Moreover, the mortality study indicates complete apoptotic arrest of cancerous cells due to the action of Vincristine drug (250 nM) after 12 h. The apoptosis occurs faster (6 h) when treated with higher concentrations (500 nM and 1 μ M). Finally, statistical parameters (cell count and Organelle structure count) are carried out at various flow speeds as a part of a large population study.

, $L_y = 125 \mu\text{m}$, and $L_z = 500 \mu\text{m}$. The ZY dimension of $500 \times 125 \mu\text{m}^2$ suggests complete cross-sectioning of the specimens flowing through all the channels simultaneously. It may be noted that the intensity profiles of the two excitation light sheets along the Z-axis are different, although the profiles along the X- and Y-axes are similar. This is because there is a difference in the beam width of the source lasers (473 nm and 532 nm) which upon focussing by the combination of cylindrical lens—objective lens produces different L_z profiles. Since the effective system PSF has a size larger than the microfluidic channel (of size $\sim 100 \times 100 \mu\text{m}^2$), this has no impact on the performance of m-iLIFE. Once the illumination PSF is characterized, the cytometry system requires the characterization of detection PSF.

The detection PSF requires calibration of point emitters (flowing fluorescent beads) at varying flow speeds (833–2490 $\mu\text{m}/\text{s}$). The corresponding PSFs along with the intensity plots are shown in Fig. 2B. The size of system PSF facilitates the sectioning of cells flowing through microfluidic channels. It is used to simultaneously interrogate multiple organelles. The next step is the determination and characterization of detection PSF for minimizing flow-induced motion blur caused by flowing specimens. This generates a collection of flow-variant PSFs that can be used for image deconvolution. Fig. 2C shows detection PSFs at a few selected flow-speeds (166–3320 $\mu\text{m}/\text{s}$), along with the intensity plots. This corresponds to a flow rate of 100–2000 nl/min. The corresponding recorded raw video is shown in Supplementary Video 1. The plots suggest two specific effects, the broadening of detection PSFs and the loss of intensity which can be attributed to low photon budget at high-speed (say, 3320 $\mu\text{m}/\text{s}$). This broadening is quantitatively shown in Fig. 2B,C, which suggests a nearly linear increase in FWHM of the detection PSF with flow rate. Relative increase is about, $S_{166} : S_{3320} = 5.85\mu\text{m} / 3.88\mu\text{m} \approx 1.5$. Post-data collection, the flow-variant PSFs are used to deconvolve the recorded sectional images (both channels) of flowing cells and reconstruct high-quality volume on the go.

The ability to interrogate cells on a variety of microfluidic chips (single and multiple channels) at high-throughput is of high commercial value. The proposed technique supports and validates such an open-ended design as shown in Fig. 3. Three different channel types are shown along with varying sizes of light sheets (marked by a yellow line). The system was tested on a known specimen such as multicolor fluorescent beads (Red Beads: 1.0 μm diameter, Ex:Em = 535 nm : 575 nm, and Green Beads: (505: 515nm, Invitrogen Inc, USA)) suspended in a solution (triple-distilled water). This image of multicolor beads (green and red beads) is shown in Fig. 3. The corresponding data showing beads in the green channel (channel 1), red channel (channel 2), and together (merged) is shown in Supplementary Video 2. The green and red beads have distinct emission spectra with a maximum of 515 nm and 575 nm, respectively. The availability of dual channel detection enables the capture of images on two different parts of the detector chip. Post recording, the beads were shift-corrected (see, Methods section) and merged together. The next step is the study of cells (both healthy and cancerous cells) using the proposed cytometry system as shown in Fig. 4. We have targeted two different organelles (Lysosomes and Mitochondria) in a cell for the present study. The lysosomes were labeled using Lysotracker (Thermofisher Scientific, USA) whereas, mitochondria were labeled using Mitotracker red (Thermofisher Scientific, USA). These fluorophores are excitable at 473 nm and 532 nm, and the emission takes place at 511 nm and 644 nm (emission maxima). The signals were obtained in different channels of the detection arm and recorded in separate regions of the detector chip. Subsequently, the images are shift-corrected and merged to obtain the multicolor sectional images. The corresponding intensity plots show the distribution of these organelles in the cells. The process is carried out for 1, 2, and 4 channel chips separately as displayed in Fig. 4. The corresponding raw video data for a single color is shown in Supplementary Video 3. To demonstrate the reconstruction quality of sectional images and volume imaging capability, the images were merged, post-deconvolution as shown in Fig. 5. The deconvolution of raw images was carried out by the flow-variant PSF and stacked together to reconstruct the cell volume as shown in Fig. 5. The corresponding multicolor 3D volumes (green channel, red channel and merged) for two sample cells is shown in Supplementary Video 4. This gives a plethora of information related to the distribution of two different organelles in cell volume for a large cell population at a relatively high throughput. The proposed *m – iLIFE* cytometry technique demonstrates multicolor volume imaging of a flowing cell with organelle-level resolution.

Finally, the developed multicolor light sheet cytometry technique is used to carry out drug treatment studies on cancerous HeLa cells as shown in Fig. 6. The cells were suspended in pure PBS (pH 7.4, 1X) after trypsinization for microfluidic analysis. No antibiotics were used in the analysis mixture after trypsinization. However, it was used during cell culture as per the developed protocols (see, Section III.E). Post cell sample preparation, the experiment was carried out that lasted 5–6 minutes and this time was enough to analyze the cells. During experimentation, the cells remained in PBS and were not affected by the PBS. As far as staining is concerned, the mitochondria and lysosomes in cells were stained using Mitotracker Red FM, and Lysotracker Green dyes (see section III.E). A comprehensive study, both at varying drug concentrations and at different time points are carried out, thereby demonstrating the capability of high-throughput investigation of a large pool of cells. Based on the available literature, concentration over a wide range (75 nM–1 μM) is used for the present study. Within the first 3 h of post-drug treatment, the cells showed disintegration of the mitochondrial network and its accumulation at the cell membrane. A similar effect on the Lysosomes (appearing as discrete dots) is also evident. The effect is clearly visible in the merged multicolor sectional images of flowing cells. The corresponding colocalization studies indicate a percentage match for both organelles, post-treatment. With the increase in time, two effects were visible, (1) organelle accumulation at the peripheral cell membrane, and (2) a relative shrink in the cell size. To access the effect of the drug, control experiments were carried out where untreated HeLa cells were flown and images were acquired as shown in Fig. 6. Mortality test shows apoptosis of a large percentage of cancer cells with the maximum occurring for >20 h (see, Fig. 6B). Another distinct advantage of the system is its ability to count both cells and organelles during flow in addition to high-resolution multicolor volume imaging (see, Fig. 6C). We noted an average count of 400 cells per minute with a maximum of about 742 cells per minute. In addition, the system allows the count of multiple organelles during flow. This is incredible considering the

availability of multicolor cell volume during flow. Such a capability facilitates the study of multiple organelles in live cells at high throughput, a feat not achieved to date. Overall, the drug treatment studies demonstrate the potential of the multicolor *iLIFE* (*m-iLIFE*) system for imaging cytometry and biomedical engineering.

Conclusion and discussion

We report the development of a new kind of multicolor flow imaging system primarily based on light sheet technology. Unlike existing techniques, *m-iLIFE* uses a single multicolor light sheet for screening cells flowing through multiple microfluidic channels. The use of a multicolor light sheet eliminates the use of hydrodynamic focusing thereby lifting several constraints (the need for sheath fluid, sequential interrogation, and poor resolution) and bringing in huge benefits (multi-organelle interrogation, volume visualization, and organelle-level resolution), potentially leading to the miniaturization of imaging cytometry system. Moreover, *m-iLIFE* facilitates the imaging of multiple organelles in parallel for multiple cells, in addition to regular tasks carried out by existing imaging cytometry systems. We expect this to have a huge impact in the fields of cell biophysics, fluorescence imaging, clinical biology, and biomedical engineering.

m-iLIFE system employs a system PSF for interrogating the sample and a dual-channel multicolor 4f widefield detection for optical sectioning. The illumination is achieved by combining two different lasers and using an integrated cylindrical lens - objective lens configuration. The resultant system PSF is characterized and critical parameters are determined (see, Fig. 2). Subsequently, the detection sub-system is characterized using a test sample (fluorescent beads of size, 1 μm). In addition, a microfluidic chip based design is employed to interrogate flowing fluorescently-labeled cells (Lysosomes labeled with Lysotracker Green, and Mitochondria labeled with Mitotracker Red)). For detection, a multicolor dual-channel single camera-based 4f system is developed (see, Fig. 1). Simultaneous detection of multiple organelles is achieved by the detection sub-system, which requires splitting of two distinct fluorescence emanating from two different organelles in the cell. Since cells are in flow, a motion blur is evident. De-blurring is a challenging task since a proper theoretical model is not available for flow-based systems. To overcome this, we used fluorescent beads as point sources, and the corresponding flow-variant PSF is determined experimentally, which is then used in the ML algorithm to deblur the recorded sectional images. The processed images are then stacked together for volume reconstruction (see, Fig. 5).

High-throughput imaging is key to the developed *m-iLIFE* system. Given the additional requirement of multi-organelle interrogation, the system employs a system PSF which is capable of counting multiple organelles and facilitates the determination of their distribution in the cell volume (see, Fig. 4). The system has shown the unique ability to record 5 sectional images at a flow-rate of 1500 nl/min, enabling near real-time multicolor volume reconstruction (see, Fig. 5). Specifically, the system allowed visualization of ~ 800 cells per minute. In addition, organelle-level resolution ($\sim 3 \mu\text{m}$) has allowed the counting of multiple organelles (mitochondria and lysosomes) (see, Fig. 6). All these factors add distinct advantages to *m-iLIFE*, both in terms of speed and multicolor interrogation. This is an achievement over the existing systems, in terms of multicolor volume imaging on the go.

It may be noted that, the cells were flown through the microfluidic channels at varying flow rates (controlled by suction-pump). On average, we observed 3–5 single cells per channel at the same time (per frame). Frequently, we observed more than one cell in the same plane and sectioned by the light sheet. In this case, lightsheet contemporary strikes more than one cell. However, we did not observe any interference or other optical aberrations in the final optical reading of the inner cellular structures. While along the propagation, the absorption of light by the specimen can produce some artifacts because of a reduction in intensity, these artifacts dominate in thick samples, but not for thin samples ($< 100 \mu\text{m}$) such as cells. In our case, the sum of the thickness of the multiple cells in the channel at the same time is less than 100 μm , and hence these artifacts can be neglected. However, interrogating thick samples requires large penetration depths that can be achieved using a diffraction-free Bessel light sheet⁵⁵. In our cases, these artifacts may be present but did not affect the image quality.

The potential of *m-iLIFE* system is accessed via drug treatment studies on cancer cells (see, Fig. 6). The studies at varying concentrations and time points indicate a ring effect indicating cell apoptosis. This is never observed in a flow-based large-scale cell population study. Specifically, cell apoptosis is observed in the first 3 h of drug (Vincristine) treatment. Further study over a longer period of time (> 12 h) strengthens the effect. While lysosomes appear discrete, mitochondria are more connected, but both appear at the cell's peripheral membrane. This suggests that the drug disintegrates the mitochondrial network and the resultant remains move to the negatively charged cell membrane, indicating the biophysical mechanism of the drug action on the cancer cell. Such an effect is not observed in untreated cells (see, Fig. 6). We noted an efficiency of $\sim 83\%$ as compared to control. An important consequence of the effect followed by cell apoptosis is critical for the potential of the drug Vincristine (also known for its effect on mitochondrial proteins) in treating/containing cancer.

So, the potential of *m-iLIFE* for carrying out critical cell physiological studies is imminent. The fact that multiple organelles can be investigated with the addition of parameter estimation, all on a single platform and in near real-time makes *m-iLIFE* a promising next-generation cytometry system. The technique is expected to advance multiple fields at the interface of cell biophysics, clinical biology, fluorescence imaging, and optical physics.

Materials and methods

Optical setup

The *m-iLIFE* imaging cytometry system has three major sub-systems: multicolor light-sheet illumination, multichannel microfluidic specimen holder, and multicolor detection subsystems.

Multicolor illumination sub-system

Two diffraction-limited colinear light sheets are generated from two independent laser lines of wavelengths, 473 nm (LRS-0473-TSM-00100-10, Laserglow, Canada) and 532 nm (Excel Laser, Quantum Lasers, UK) for exciting the fluorophore-labeled cells passing through an array of microfluidic channels. Beam-1($\lambda = 473\text{nm}$ and diameter = 1.5mm) and beam-2($\lambda = 532\text{nm}$ and diameter = 1.5mm) are combined using a beam-combiner (high-pass DC-505, Thorlabs, USA) and expanded 5X times using a beam-expander (consists of two biconvex lenses, $f_1 = 25 \text{ mm}$ and $f_2 = 125 \text{ mm}$) to fill the back-aperture of the cylindrical lens. After passing through the cylindrical lens ($f = 125 \text{ mm}$, Edmund Optics, Singapore), the light is focused on the back aperture of the illumination objective lens (Olympus 10X, 0.30 NA) to generate diffraction-limited light sheets. This collinear diffraction-limited light sheet is the illumination PSF.

μ -chip and microfluidic flow platform

A Y-shaped microfluidic channel array was used to flow cells and fluorescent beads. The microfluidic chip is firmly held by a custom-made chip holder and was positioned precisely using an XYZ translator with respect to the light sheet at an angle of 45°. This arrangement allows easy calibration and positioning for precision optical sectioning of the μ -channel array, which consists of four channels, each with a cross-section of $100 \times 100\mu\text{m}^2$. The microfluidic chip has an inlet connected to a sample reservoir containing the cells, while the outlet is linked to a flow pump. The pump operated in suction mode and all the operations were controlled by computer-based interface software. Both the beads and cells were flown through the channel array simultaneously and captured through the multicolor detection subsystem.

Multi-color detection

HeLa cells were stained with Lysotracker green DND-26 ($\lambda_{em1} = 525 \text{ nm}$) and MitoTracker red FM ($\lambda_{em2} = 650 \text{ nm}$) to label the lysosomes and mitochondrial network, respectively. The detection objective collects the fluorescence signal from the HeLa cells flowing through the micro-channels and directs it to the notch filters to eliminate the illumination light. The light is then allowed to pass through an auto-tunable lens and split into two separate signals by placing a high-pass dichroic filter (cutoff wavelength = 600nm, purchased from Edmund Optics) at 45° in the path of the beam. Both the signals are steered by the mirror to focus on the different parts of sCMOS detector chip (pixel size = $6.5 \mu\text{m} \times 6.5 \mu\text{m}$, chip size in pixels = 2048×2048). A set of band-pass filters is introduced in the path of both signals to cut off the background and stray light. For transmitted light, the band-pass filter range is 641/80 nm (OD = 6.0, purchased from Edmund Optics), whereas reflected light is filtered out by band-pass filter 525/50 nm (purchased from Chroma).

Point spread function, data acquisition and image processing

The images were recorded on a single Andor sCMOS Zyla 4.2 camera (pixel size = $6.5 \mu\text{m}$ & *Quantum Efficiency* = 82%, $2048 \times 2048 \text{ pixels}$). The fluorescence from channel 1 was recorded in one half of the chip and fluorescence from channel 2 was projected on the other half of the sCMOS chip. The images are recorded in .tif format in Solis software compatible with the Zyla 4.2 camera and converted to tiff format as image sequences.

System PSF for m – iLIFE

The illumination PSF for the proposed m-iLIFE system is a superposition of two independent PSFs (light-sheet PSFs at 473 nm and 532 nm). The PSFs are chosen to efficiently excite two different fluorophores (here, MitoTracker red FM ($\lambda_{em2} = 650 \text{ nm}$) for labeling mitochondria and Lysotracker green DND-26 ($\lambda_{em1} = 525 \text{ nm}$) for labeling lysosomes). The system requires the alignment of individual light sheets in the specimen plane to realize overlapping light sheets. This enables the interrogation of multiple organelles in parallel. A high degree of alignment (with a PSF overlap of 88.81%) is ensured before imaging the cells.

The detection PSF is essentially a widefield dual-channel 4f system, where the fluorescence from the specimen is collected by the detection objective. This is followed by filtering to remove the excitation light and then focused by the tube lens to the detector. A dichroic mirror is placed to separate the spectrally distinct fluorescence emitted by two different organelles. The light then passes through a series of mirrors which directs it to two different regions of the camera/detector chip. On its way, a couple of additional filters are placed to reduce the background and stray light. The image which consists of two sub-images obtained from two different channels is simultaneously recorded and sent for further processing. The picture of actual *m – iLIFE* imaging cytometry system is shown in Fig. S1 and discussed in Supplementary Note 1.

Overall, the system PSF ensures multicolor imaging in imaging flow cytometry with sub-cellular resolution.

Flow-variant point spread function and deconvolution

The fact that flow induces distortions in system PSF and degrades the overall image quality calls for image processing techniques. To suppress these flow-induced aberrations, we experimentally determine flow-variant PSF at each flow rate and use the same for image deconvolution.

To characterize the flow variant PSF, beads are used as the fluorescent point emitters. They were flown through the microfluidic channels to record flow variant PSF. The recorded PSF is used to deconvolve the recorded images and reconstruct cell volume. Using bivariate Gaussian fitting, the parameters associated with the flow-induced elongated PSF are extracted using MATLAB 2022a. The deconvolution is carried out using an inbuilt maximum likelihood (ML) algorithm employing flow-variant PSF. ML algorithm use the likelihood function (here, $L(g/f)$) as a cost function and maximizes the same i.e,

$$\max_{f>0} L(g \mid f) = \max_{f>0} \left[\prod_{j=1}^n e^{-(Af)_j} \frac{(Af)_j^{g_j}}{g_j!} \right] \quad (1)$$

where, g is the recorded image of the object o flowing through the microfluidic channel with A the convolution operator expressed as, $Af = h \otimes f$. ML algorithm are standard operations in Matlab and the same is used to determine the maximum likelihood estimate of the recorded sectional images.

The sectional images obtained from both channels are recorded on the camera chip, with the left half for channel 1 and the right half for channel 2. Subsequently, the images are deconvolved, shift-corrected, and stacked to reconstruct the 3D volume image. Specifically, the recorded data is deconvolved with flow variant PSF to reduce the effect of flow-induced motion blur (see, section III.B), which is then followed by shift-correction determined during the calibration experiment and correlation study (see, Supplementary Note 2). Finally, the images are stacked together to reconstruct 3D volume image of the cells flowing through the microfluidic channels. To automate the entire process for rapid volume reconstruction, a combination of Matlab and ImageJ software are used.

Design and development of microfluidics chip

Microfluidic channels used for flowing specimens in a $m - iLIFE$ system were fabricated using a master mold. The microfluidic chip fabrication is carried out at the nanofabrication facility at the Centre for Nanoscience and Engineering at the parent institute (Indian Institute of Science, Bangalore, India). The process begins by designing the channels on Clewin4 Software in .gbr file format. This pattern is then printed on a negative photolithographic mask. Subsequently, the Y-type channels of various dimensions were then patterned onto the silicon wafer using a standard photolithography technique using a negative photoresist SU-8 2100. The depth corresponding to each channel on the silicon mold is 100 μm , while the thickness and the separation between consecutive channels are achieved as required by the experiment. The mixture of polydimethylsiloxane (PDMS) and its curing agent from Dow Corning's Sylgard 184 elastomer are mixed thoroughly in the ratio of 10:1. Furthermore, it was poured on the master to get the required pattern in PDMS following the protocol discussed in Ref.¹⁶. A net mixture amount of 33 g is degassed with a vacuum pump until the air bubbles are removed. The degassed mixture is gently poured on the top of the master mold and is cured in a hot oven at 60 °C for 3–4 h. Cured PDMS is peeled off from the master mold, and useful regions are extracted from it by cutting. Thus, a replica of the microchannels on the PDMS blocks is obtained. Inlets and outlets are punched with a 1.0 mm diameter PDMS puncher and cleaned with isopropanol and acetone. The washed PDMS chip and bonding glass (0.15 mm thickness) are plasma-cleaned for 5 minutes. Thereafter, PDMS is placed on the top of coverslips, followed by baking on the hotplate for 5 min at 90 °C. Post fabrication, holes of the dimension of external tubes were punched at both ends of the Y-type channel array (consisting of four inter-connected channels). Using microfluidic Teflon tubing (inner diameter of 0.5 mm) reservoir is connected to the inlet, and the outlet is joined to the flow pump. The flow is controlled in the range of 166 to 3320 $\mu\text{m}/\text{s}$ using an external pump (operated in withdrawal mode).

Here, the microfluidic chip is designed with PDMS and the glass coverslip (Fig. 1). As shown in the figure, the light sheet strikes through the air-glass interface to interact with the specimen flowing through channels and does not penetrate PDMS directly anywhere. The same is true for the collection of fluorescence emitted by the specimen. Here, the PDMS is responsible for holding the specimen in the microfluidic channels. Moreover, the optical issues for the air-glass interface are minimal and can be neglected. We did not observe any visible changes in the reconstructed volume due to the coverglass-PDMS interface.

Sample preparation and cell labelling protocol

Fluorescent beads

Fluorescent Beads are used as point emitters in fluorescence measurements in microscopy and spectroscopy. The beads are used for calibration and as test specimens for $m - iLIFE$ imaging system. It has very well-defined absorption and emission spectra and is available commercially with different spectral ranges.

a. *Red-Niel Fluospheres* 1 μl of carboxylate modified micro spheres (Invitrogen, USA) of 1 μm diameter are suspended in 1 ml distilled water. After a thorough mixing of microsphere in water, it was loaded in the reservoir, and flow experiments were performed.

b. *Yellow-Green Fluospheres* From FluoSpheresTM Biotin-Labeled Microspheres (Invitrogen, USA) of size 1.0 μm yellow-green fluorescent (Ex/Em=505/515 nm, 1% solids), the sample was prepared in the same way as we did for Niel red beads. We mix 1 μl yellow-Yellow-green beads with 1 ml water. After thorough mixing, the beads (suspended in PBS) were loaded in the reservoir.

Mammalian cell lines and staining protocols

Simultaneous Lysosomal and Mitochondrial staining

HeLa cells are cultured up to 90 percent confluence in the T25 flask. To label the mitochondrion and lysosomes, LysoTracker Green and MitoTracker Red FM are used.

Preparation of stock solution of Lysotracker Green

From the main stock of Lysotracker Green of concentration 1 mM in DMSO, we prepared the solution in DMEM of various concentrations. Finally, we optimize the concentration of dye to 100 nM for staining.

Preparation of stock solution of MitoTracker Red FM

The main stock of MitoTracker Red FM of 1 mM concentration dissolved in DMSO is used to prepare the dye solution to stain the mitochondrial network in HeLa cells. The solution is diluted to an optimized concentration of 175 nM in DMEM and the same is used in experiments.

Culture of cell line and maintenance

HeLa cells (human cervical carcinoma cell line) were used for the experiment. It was grown as monolayers in Dulbecco's modified minimal Eagle's medium (DMEM) (Gibco, Thermo Fisher Scientific) supplemented with 10% FBS (Gibco, Thermo Fisher Scientific) and 1% penicillin-streptomycin solution (Gibco, Thermo Fisher Scientific). The general cell culture process was carried out in a biosafety cabinet (Class II Forma series 381, ThermoFisher). The cells were thawed, and standard running culture was maintained in an incubated humidified chamber at 37°C and 5% CO₂ (CO₂-incubator, Thermo Scientific). After 2 passages, the cells were prepared for the experiment. A hemocytometer is used to count cells after every passage, and approximately 100,000 cell count was maintained. The cells were passaged every 2–3 days to maintain healthy cell lines.

Next, we washed the cells with PBS to remove the debris from HeLa cells. First, we label the lysosomes. For this, we incubated the cells with the prepared solution of LysoTracker green (100 nm concentration) for up to 20 min at 37°C. After incubation, we removed this LysoTracker solution and washed the cells with PBS. Washed cells are again incubated with MitoTracker Red FM solution (175 nM concentration) for 30 min at 37°C to stain the mitochondrion. From incubated cells, the dye solution is separated and again washed with PBS to remove the dyes properly. We add the trypsin solution to the cells and incubate for 4 min to detach the HeLa cells from the flask surface. After completing the incubation period, detached cells with trypsin are shifted into a centrifuge tube and centrifuged for up to 5 min at 5000 rpm. Now the cells are settled in the bottom of the tube. Trypsin solution is removed from the tube, and the pallet is thoroughly mixed with PBS for imaging.

Data availability

The data that support the findings of this study are available from the corresponding author upon request.

Received: 14 February 2024; Accepted: 19 September 2024

Published online: 11 October 2024

References

1. Mondal, Partha P. A perspective on light sheet microscopy and imaging: Applications across the breadth of applied physics and biophysics. *Appl. Phys. Lett.* **119**, 160502 (2021).
2. Stelzer, Ernst H. K. et al. Light sheet fluorescence microscopy. *Nat. Methods Prim.* **1**, 73 (2021).
3. Huisken, J. et al. Optical sectioning deep inside live embryos by selective plane illumination microscopy. *Science* **305**, 1007–1009 (2004).
4. Keller, P. J. et al. Reconstruction of zebrafish early embryonic development by scanned light sheet microscopy. *Science* **322**, 1065 (2008).
5. Holekamp, T. E., Turaga, D. & Holy, T. E. Fast three-dimensional fluorescence imaging of activity in neural populations by objective-coupled planar illumination microscopy. *Neuron* **57**, 661 (2008).
6. Migliori, B. et al. Light sheet theta microscopy for rapid high-resolution imaging of large biological samples. *BMC Biol.* **16**, 57 (2018).
7. Chen, B. C. et al. Lattice light-sheet microscopy: Imaging molecules to embryos at high spatiotemporal resolution. *Science* **346**, 1257998 (2014).
8. Fan, Y.-J., Hsieh, H.-Y., Tsai, S.-F., et al. *Lab Chip 21, Microfluidic Channel Integrated with a Lattice Lightsheet Microscopic System For Continuous Cell Imaging* 344–354 (2021).
9. Mohan, K., Purnapatra, S. B. & Mondal, P. P. Three dimensional fluorescence imaging using multiple light-sheet microscopy. *PLoS ONE* **9**, e96551 (2014).
10. Mondal, P. P., Dilipkumar, S. & Mohan, K. Efficient generation of diffraction-limited multi-sheet pattern for biological imaging. *Opt. Lett.* **40**, 609–612 (2015).
11. Marc, L. et al. Light field microscopy. *ACM Trans. Graph.* **25**, 924 (2006).
12. Broxton, M. et al. Wave optics theory and 3-D deconvolution for the light field microscope. *Opt. Express* **21**, 25418 (2013).
13. Wenhao, L. & Jia, S. wFLFM: Enhancing the resolution of Fourier light-field microscopy using a hybrid wide-field image. *Appl. Phys. Express* **14**, 012007 (2021).
14. Regmi, R., Mohan, K. & Mondal, P. P. Light sheet based imaging flow cytometry on a microfluidic platform. *Microsc. Res. Tech.* **76**, 1101 (2013).
15. Raju, R., Kavya, M. & Mondal, P. P. High resolution light-sheet based high-throughput imaging cytometry system enables visualization of intra-cellular organelles. *AIP Adv.* **4**, 097125 (2014).
16. Kumar, P., Joshi, P., Basumatary, J. & Mondal, Partha P. Light sheet based volume flow cytometry (VFC) for rapid volume reconstruction and parameter estimation on the go. *Sci. Rep.* **12**, 78 (2022).
17. Mondal, P. P. The expanding horizon of light sheet technology. *iScience* **6**, 2 (2021).
18. Mohan, K. & Mondal, Partha P. Spatial filter based light-sheet laser interference technique for three-dimensional nanolithography. *Appl. Phys. Lett.* **106**, 083112 (2015).
19. Mohan, K. & Mondal, P. P. Experimental observation of nano-channel pattern in light sheet laser interference nanolithography system. *Rev. Sci. Instrum.* **87**, 066107 (2016).
20. Mohan, K. & Mondal, Partha P. MRT Letter: Two-photon excitation-based 2pi Light-sheet system for nano-lithography. *Microsc. Res. Tech.* **78**, 1–7 (2015).
21. Mohan, K., Tyagi, A. & Mondal, Partha P. Multi-sheet light enables optical interference lithography. *Rev. Sci. Instrum.* **89**, 066106 (2018).
22. Mohan, K. & Mondal, Partha P. Experimental realization of sub-micron patterning using counter-propagating interfering lightsheets (iCLASS). *OSA Cont.* **3**, 668–675 (2020).
23. Golub, I., Chebbi, B. & Golub, J. Toward the optical “magic carpet”: Reducing the divergence of a light sheet below the diffraction limit. *Opt. Lett.* **40**, 5121–5124 (2015).
24. Laskin, A. & Laskin, V. Beam shaping to generate uniform laser light sheet and linear laser spots. *Proc. SPIE* **8843**, 88430C (2013).

25. Aakhte, M., Akhlaghi, E. A. & Muller, H. A. SSPIM: A beam shaping toolbox for structured selective plane illumination microscopy. *Sci. Rep.* **8**, 10067 (2018).
26. Pai, D. Z. Plasma-liquid interfacial layer detected by in situ Raman light sheet microspectroscopy. *J. Phys. D* **54**, 355201 (2021).
27. Regmi, R., Mohan, K. & Mondal, Partha P. Light sheet based imaging flow cytometry on a microfluidic platform. *Microsc. Res. Tech.* **76**, 1101 (2013).
28. Chelur, R. K. et al. Integrated light-sheet imaging and flow-based enquiry (iLIFE) system for 3D in-vivo imaging of multicellular organism. *Appl. Phys. Lett.* **111**, 243702 (2017).
29. Mondal, P. P. iLIFE: The next generation imaging cytometry: A boon to health-care and medicine. *iScience* **3**, 1 (2018).
30. Siedentopf, H. & Zsigmondy, R. Über Sichtbarmachung und Größenbestimmung ultramikroskopischer Teilchen, mit besonderer Anwendung auf Goldrubiingläser. *Ann. Phys.* **315**, 1–39 (1902).
31. Voie, A. H., Burns, D. H. & Spelman, F. A. Orthogonal-plane fluorescence optical sectioning: Three-dimensional imaging of macroscopic biological specimens. *J. Microsc.* **170**, 229–236 (1993).
32. Huisken, J., Swoger, J., Del Bene, F., Wittbrodt, J. & Stelzer, E. H. Optical sectioning deep inside live embryos by selective plane illumination microscopy. *Science* **305**, 1007–1009 (2004).
33. Keller, P. J., Schmidt, Annette D., Wittbrodt, Joachim & Stelzer, Ernst HK. Reconstruction of zebrafish early embryonic development by scanned light sheet microscopy. *Science* **322**, 1065 (2008).
34. Keller, P. J. et al. Fast, high-contrast imaging of animal development with scanned light sheet-based structured-illumination microscopy. *Nat. Methods* **7**, 637–642 (2010).
35. Lau, A. K. S., Shum, H. C., Wong, K. K. Y. & Tsia, K. K. Optofluidic time-stretch imaging: An emerging tool for high-throughput imaging flow cytometry. *Lab Chip* **16**, 1743–1756 (2016).
36. Miura, T. et al. On-chip light-sheet fluorescence imaging flow cytometry at a high flow speed of 1 m/s. *Biomed. Opt. Express* **9**(7), 3424–3433 (2018).
37. Collier, B. B., Awasthi, S., Lieu, D. K. & Chan, J. W. Non-linear optical flow cytometry using a scanned, bessel beam light-sheet. *Sci. Rep.* **5**, 10751 (2015).
38. Mahjoubfar, A., Chen, C., Niazi, K. R., Rabizadeh, S. & Jalali, B. Label-free high-throughput cell screening in flow. *Biomed. Opt. Exp.* **4**, 1618–1625 (2013).
39. Jiang, H. et al. Droplet-based light-sheet fluorescence microscopy for high-throughput sample preparation, 3-D imaging and quantitative analysis on a chip. *Lab Chip* **17**, 2193–2197 (2017).
40. Bouchard, M. B. et al. Swept confocally-aligned planar excitation (SCAPE) microscopy for high-speed volumetric imaging of behaving organisms. *Nat. Photon.* **9**, 113–119 (2015).
41. Martin, Chris, Li, Tianqi, Hegarty, Evan & Zhao, Peisen. Sudip Mondal and Adela Ben-Yakar, Line excitation array detection fluorescence microscopy at 0.8 million frames per second. *Nat. Commun.* **9**, 4499 (2018).
42. Joshi, P., Kumar, P., Aravindh, S., Varghese, J. M. & Mondal, Partha P. Fluorescence-based multifunctional light sheet imaging flow cytometry for high-throughput optical interrogation of live cells. *Commun. Phys.* **7**, 25 (2024).
43. Hiramatsu, K. et al. High-throughput label-free molecular fingerprinting flow cytometry. *Sci. Adv.* **5**, eaau0241 (2019).
44. Han, Y., Gu, Y., Zhang, A. C. & Lo, Y. H. Review: Imaging technologies for flow cytometry. *Lab Chip* **16**, 4639–4647 (2016).
45. Chang, S., Serena, K., Karen, S. & Gyongyi, S. Impaired expression and function of toll-like receptor 7 in hepatitis C virus infection in human hepatoma cells. *Hepatology* **51**, 35–42 (2010).
46. Maguire, O., Collins, C., O'Loughlin, K., Miecznikowski, H. & Minderman, H. Quantifying nuclear p65 as a parameter for NF-B activation: Correlation between ImageStream cytometry, microscopy, and Western blot. *Cytometry A* **79**, 461–469 (2011).
47. Begum, J. et al. A method for evaluating the use of fluorescent dyes to track proliferation in cell lines by dye dilution. *Cytometry A* **83**, 1085–1095 (2013).
48. Riordon, J. et al. Deep learning with microfluidics for biotechnology. *Trends Biotechnol.* **37**, 310–324 (2019).
49. Isozaki, A. et al. AI on a chip. *Lab Chip* **17**, 3074–3090 (2020).
50. Doan, M. et al. Carpenter Holger Hennig, diagnostic potential of imaging flow cytometry. *Trend. Biotech.* **36**, 649–652 (2018).
51. Lin, J.-R., Fallahi-Sichani, M. & Sorger, P. K. Highly multiplexed imaging of single cells using a high-throughput cyclic immunofluorescence method. *Nat. Commun.* **6**, 8390 (2015).
52. Lin, J.-R. et al. Highly multiplexed immunofluorescence imaging of human tissues and tumors using t-CyCIF and conventional optical microscopes. *eLife* **7**, e31657 (2018).
53. Goltsev, Y. et al. Deep profiling of mouse splenic architecture with CODEX multiplexed imaging. *Cell* **174**, 968–81 (2018).
54. Bodenmiller, B. Multiplexed epitope-based tissue imaging for discovery and healthcare applications. *Cell Syst.* **2**, 225–38 (2016).
55. Meinert, T. & Rohrbach, A. Light-sheet microscopy with length-adaptive Bessel beams. *Biomed. Opt. Exp.* **10**, 670–681 (2019).
56. Mondal, Partha P. Book: *Light Sheet Microscopy and Imaging* (AIP Publishing, 2021).
57. Stelzer, Ernst H. K. et al. Light sheet fluorescence microscopy. *Nat. Rev. Methods Prim.* **1**, 73 (2021).

Acknowledgements

The authors acknowledge financial support from, Department of Biotechnology & DST, New Delhi, India, and the parent institute (Indian Institute of Science, Bangalore, India). PPM conceived the idea. PK and PPM carried out the experiment. PK prepared the samples. PPM wrote the paper by taking inputs from PK.

Declarations

Conflicts of Interest

The authors declare no conflicts of interest.

Additional information

Supplementary Information The online version of this article (<https://doi.org/10.1038/s41598-024-73667-3>) contains supplementary material, which is available to authorized users.

Correspondence and requests for materials should be addressed to P.P.M.

Reprints and permissions information is available at www.nature.com/reprints.

Publisher's note Springer Nature remains neutral with regard to jurisdictional claims in published maps and institutional affiliations.

Open Access This article is licensed under a Creative Commons Attribution-NonCommercial-NoDerivatives 4.0 International License, which permits any non-commercial use, sharing, distribution and reproduction in any medium or format, as long as you give appropriate credit to the original author(s) and the source, provide a link to the Creative Commons licence, and indicate if you modified the licensed material. You do not have permission under this licence to share adapted material derived from this article or parts of it. The images or other third party material in this article are included in the article's Creative Commons licence, unless indicated otherwise in a credit line to the material. If material is not included in the article's Creative Commons licence and your intended use is not permitted by statutory regulation or exceeds the permitted use, you will need to obtain permission directly from the copyright holder. To view a copy of this licence, visit <http://creativecommons.org/licenses/by-nc-nd/4.0/>.

© The Author(s) 2024